ACS Sustainable Chemistry & Engineering

Research Article

pubs.acs.org/journal/ascecg

Synthesis and Characterization of Halloysite–Cyclodextrin Nanosponges for Enhanced Dyes Adsorption

Marina Massaro,[†] Carmelo G. Colletti,[†] Giuseppe Lazzara,*[,‡] Susanna Guernelli,[§] Renato Noto,[†] and Serena Riela*[,†]

[†]Dipartimento STEBICEF, Sez. Chimica, Università degli Studi di Palermo, Viale delle Scienze, Ed. 17, 90128 Palermo, Italy
[‡]Dipartimento di Fisica e Chimica, Università degli Studi di Palermo, Viale delle Scienze, Ed. 17, 90128 Palermo, Italy
[§]Dipartimento di Chimica "G. Ciamician", Università degli Studi di Bologna, Via S. Giacomo 11, 40126 Bologna, Italy

Supporting Information

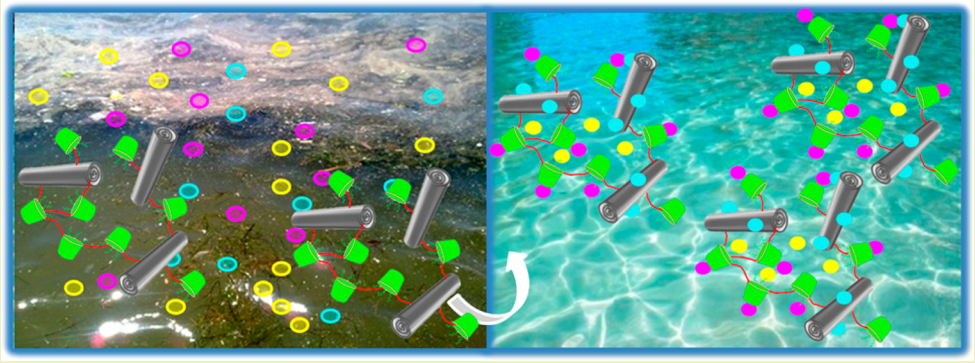

ABSTRACT: Inorganic–organic nanosponge hybrids based on halloysite clay and organic cyclodextrin derivatives (HNT-CDs) were developed by means of microwave irradiations in solvent-free conditions. The HNT-CDs nanomaterials characterized by FT-IR, TGA, BET, TEM, SEM, DLS, and ζ-potential have showed a hyper-reticulated network which possesses both HNT and cyclodextrin peculiarities. The new HNT-CDs nanosponge hybrids were employed as nanoadsorbents, first choosing Rhodamine B as the dye model, and furthermore for the removal of some cationic and anionic dyes, under different pH values (1.0, 4.54, and 7.4). The collected results showed that the pH solution as well as the electrostatic interactions affect the adsorption process. Factors controlling the adsorption process were discussed. The experimental adsorption equilibrium and kinetic data were best described by the Freundlich isotherm model. Excellent adsorption efficiency for cationic dyes were observed with respect to anionic ones. The results suggest that HNT-CDs nanosponge hybrids are a good nanoadsorbent for selective adsorption of cationic dyes with respect to the anionic ones from aqueous solutions.

KEYWORDS: *Halloysite, Nanosponges, Cyclodextrin, Bioremediation*

INTRODUCTION

In the last years, mesoporous materials have become attractive due to their peculiar chemical characteristics, such as moderate pore size (within 2–50 nm diameter) and large specific surface area, that increase their applications in several fields such as adsorption, catalysis, and so on.[1] The interest for these kinds materials is mainly due to the fact that they generally are low cost, environmentally friendly, and available in large scale since they are recovered from natural sources. In this context, nanoporous minerals such as zeolite, bentonite, and montmorillonite[2,3] have shown good promise to replace the commonly used mesoporous materials.

Halloysite nanotubes (HNTs) are alumino-silicate clay with a predominantly hollow tubular structure in the submicron range. Compared to other nanoparticles such as organic carbon nanotubes, this kind of inorganic tube is naturally occurring, cheap, abundantly available, and bio-[4,5] and eco-compatible.[6] Chemically, HNTs are constituted by siloxane groups on the external surface, while the aluminol groups are located in the inner lumen.[7] Because of this peculiar chemical composition, the external surface of halloysite is easily functionalized by covalent grafting of silane groups which increases HNT application fields; moreover, the positively charged inner lumen allows for encapsulating negative- or electron-rich molecules.[8] HNTs have been used as filler for polymer[9] or hydrogel matrices,[10] drug carrier[11,12] and delivery,[13,14] and catalyst support,[15,16] as well as absorbents.[17,18]

Recently, composite materials constituted by inorganic–organic hybrids have attracted considerable attention since they combine the organic and inorganic characteristics within a

Received: December 28, 2016
Revised: February 3, 2017
Published: February 14, 2017

DOI: 10.1021/acssuschemeng.6b03191
ACS Sustainable Chem. Eng. 2017, 5, 3346–3352

single molecular-scale composite.[19] Generally, the organic moieties of the hybrids possess toughness, good elasticity, low density, and formability, whereas the inorganic components are stiff, hard, and thermally stable. Therefore, based on the combination of organic and inorganic properties, the hybrid nanomaterials are employed in a wide range of applications, such as removal of environmental pollutants.[20]

Presently, several materials are employed as adsorbent for organic dyes, such as bentonite, kaolin, and titania, as well as cyclodextrin nanosponges.[21−24]

Herein, we report a new class of inorganic−organic nanosponge hybrids obtained by the combination of the inorganic halloysite clay and organic cyclodextrin derivatives (HNT-CDs) with potentially complementary binding ability and additional nanochannels formed by the cross-link between CDs and HNT (Figure 1). The new nanosponge hybrids were

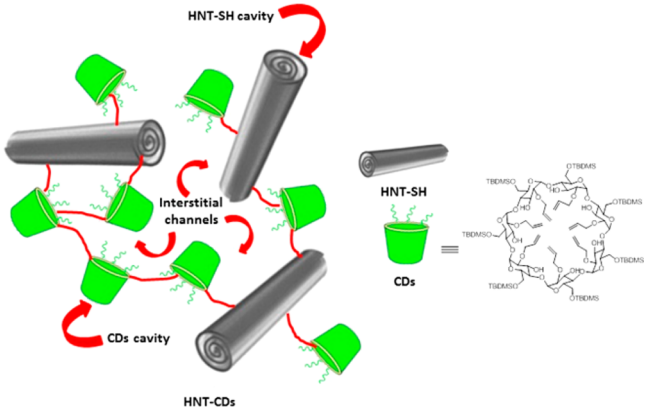

Figure 1. Cartoon representation of HNT-CDs nanosponge hybrids.

extensively characterized by FT-IR spectroscopy, thermogravimetric and BET analyses, TEM and SEM investigations, and dynamic light scattering and ζ-potential measurements. Because of these techniques, we deduce the formation of a hyper-reticulated network which possesses both HNT peculiarities and cyclodextrin characteristics. Finally, the performance of HNT-CDs nanosponges applied in organic dyes adsorption from an aqueous medium was evaluated choosing Rhodamine B (RB) as the dye model. Furthermore, the scope and feasibility of the hybrid with a wide range of organic dyes was also investigated. The method put forward the application of halloysite composite materials in the development of future efficient absorbents.

RESULTS AND DISCUSSION

The starting scaffolds HNT-SH and βCDs can be prepared by means procedures reported elsewhere.[25] As previously reported,[26] halloysite nanotubes were reacted with an excess of 3-mercaptopropyltrimethoxysilane in solvent-free conditions under microwave irradiation, affording HNT-SH, which represents a versatile starting point for subsequent functionalization. After workup, the amount of organic moiety grafted on the HNT external surface was estimated by TGA to be ca. 1 ± 0.1 wt %. The synthesis of HNT-CDs was carried out by AIBN-catalyzed polymerization of heptakis-6-(*tert*-butyldimethylsilyl)-2-allyloxy-β-cyclodextrin to HNT-SH by means of a thiolene reaction (Scheme 1).

For this synthesis, the reactants were mixed in different proportions (Table 1), and the different percentage of CDs in the obtained composite materials was determined by TGA from the residual mass upon degradation (Table 1).[25] Since the cyclodextrin is added in excess relative to the moles of −SH groups, the double bonds that do not react in the thiolene reaction can undergo a self-addition reaction, leading to the formation of a cyclodextrin cross-linked network. Therefore, due to the peculiar reticulated structure of the hybrid materials so obtained, constituted by a network of supramolecular host units joined by means of suitable cross-linkers, the hybrid polymer obtained could be considered a sort of nanosponge.[27−29]

On the basis of the stoichiometric ratios, it should be considered that an excess of unreacted allyloxy groups could be present, and they could be able to undergo further functionalizations. The polymerization was carried out in a microwave oven for an irradiation time of 1 h at 100 °C in solvent-free conditions. Then, the obtained nanomaterials were isolated by subsequent washings with CH_2Cl_2 and CH_3OH in order to remove the catalyst and some residual unreacted reagents.

Hereafter, the two different HNT-CD nanosponge hybrids are indicated as HNT-CD (20%) or HNT-CD (40%).

Compared to pristine HNT,[25] the HNT-CDs (40%) nanosponge hybrid exhibits the vibration bands for C−H stretching of methylene groups around 2980 cm^{-1} and a broad and wide band around 3000 cm^{-1} due to the −OH groups of cyclodextrin (see Figure S1). These findings provide evidence for the presence of organic moieties in the new material. Moreover, it is interesting to notice that little signals at ca. 1700 and 1418 cm^{-1} are still present in the spectrum, indicating that not all the reactive functional groups in the starting reactants actually happened to react. This may be a consequence of the hyper-reticulated nature of the hybrid polymers obtained. Steric hindrances and strains, indeed, might prevent some of the reacting groups to achieve the minimum arrangement requirements needed for the polymerization process to occur.

Thermogravimetric analysis evidenced a peculiar pyrolysis process of CDs nanosponges in the presence of HNT. Namely, the organic material degraded almost completely in a single step at ca. 327 °C that is coincident with the degradation temperature of β-CD,[30] the presence of HNT generates a two-step degradation pattern with maximum degradation rates at 265 and 360 °C, respectively. It should also be noted that the degradation at lower temperature is enhanced in the presence of larger HNT amounts (Figure 2). These findings can be explained by involving a change in the degradation mechanism of CDs nanosponges being split into two consecutive or parallel reactions.[31] To clarify the effect of HNTs on the CDs degradation mechanism, the heating rate was changed for the HNT-CDs (40%) (SI) sample, and the obtained results indicate that HNTs generate a two-step degradation mechanism rather than a catalytic degradation alternative pattern.

SEM images of the HNT-CDs (40%) nanosponge are given in Figure 3a. As known, pristine HNTs (p-HNTs) show a long fibrous morphology with a length of 0.5−1 μm and outer diameter of about 100 nm (SI).[32] After functionalization, it seems clear that the tubular shape of halloysite is preserved, and the HNT-CDs hybrid presented a different morphology as compared with p-HNTs. The HNT-CDs hybrid still shows a long-range rod shape with the diameter increasing to about 170 nm. Moreover, the hybrid shows a rather compact structure where the HNT seems glued together with a smooth surface that indicated the presence of an organic layer.

DOI: 10.1021/acssuschemeng.6b03191
ACS Sustainable Chem. Eng. 2017, 5, 3346−3352

Scheme 1. Schematic Representation of Synthesis of HNT-CDs Nanosponge Hybrid

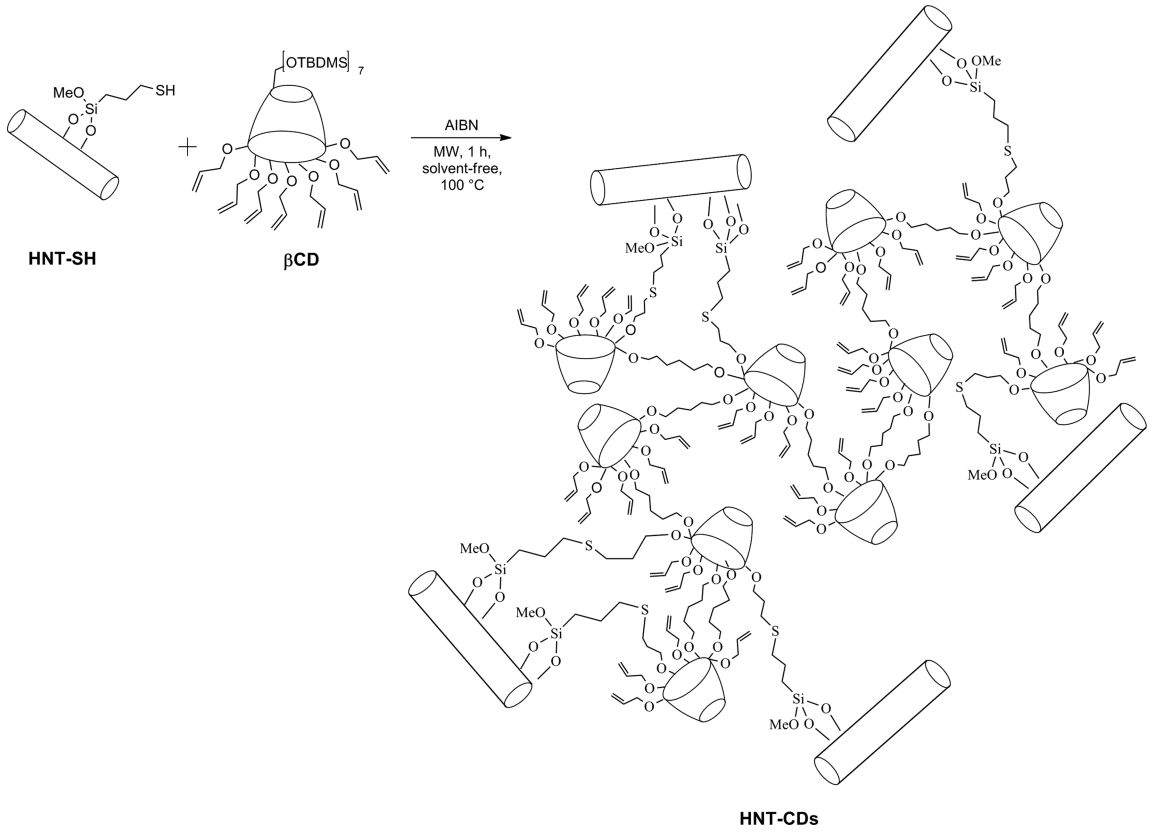

Table 1. Reactant Ratios and Mass Yields for HNT-CDs Nanosponge Hybrids

reactants	HNT-CDs products	
HNT (mg)	200	200
CD (mg)	300	150
HNT:CD ratio	1:1.5	1.5:1
% loading (CD on HNT)[a]	40	20

[a]Estimated by TGA.

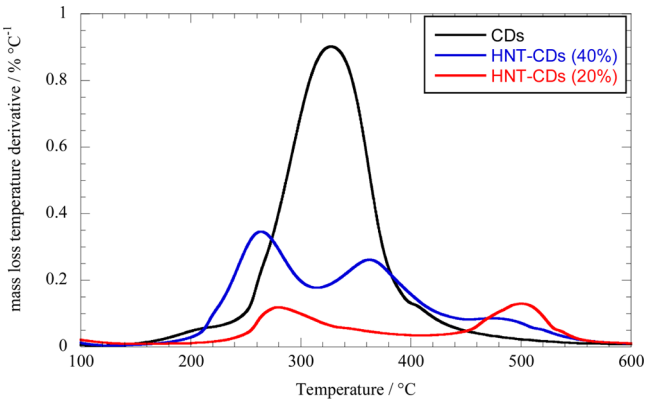

Figure 2. Differential thermal analysis curves for HNT-CD hybrid and CD polymers.

According to the TEM images (Figure 3b), the HNT-CDs hybrid (40%) shows the typical nanorod-shaped structure of HNTs. The hybrid exhibits the characteristic hollow tubular structure of halloysite as a shell with a cyclodextrin core (indicated by arrows in the Figure 3b).[33] The increased thickness of the hybrid with respect to pristine nanotubes takes into account the formation of the network after the reaction.[34]

To confirm the formation of the reticulated structure, the diffusion dynamics in water of the HNT-CDs (40%) nanosponge hybrid was characterized by dynamic light scattering (DLS). Measurements of the particle size using DLS reveal a translational average diffusion coefficient of the HNT-CDs nanosponges of 3.24×10^{-14} m^2 s^{-1} that is smaller than the value for p-HNTs in water (9.4×10^{-13} m^2 s^{-1}); this result is consistent with the formation of a polymer-like network where HNT are incorporated after the reaction with cyclodextrin units. Although the diffusion behavior is strongly altered, the surface charge in the hybrid is not significantly altered as expected for nonionic functionalization (ζ-potential = -25 ± 1 mV).[34]

The morphological properties of the HNT-CDs (40%) hybrid, in terms of specific surface area (BET), mean pore size distribution (BJH), and cumulative pore volume, were determined by N_2 adsorption/desorption measurements and are listed in Table 2. The HNT-CDs nanosponge hybrid shows a surface area of 19.9 m^2 g^{-1}, slightly smaller than that of starting pristine halloysite (22.1 m^2 g^{-1}).[34] The slight decrease in the specific surface area, observed for the new polymeric hybrid, takes into account the small degree of organosilane loading on HNT surface. The pore size of the HNT-CDs hybrid is greater than that of p-HNT as a result of the formation of a reticulated structure that could form additional channels in the hybrid polymer mesh.[35] The porous structure makes the hybrid polymer a promising material that could act as a nanosponge for dye adsorption.

Swelling Properties of HNT-CD Nanosponge Hybrid. Since swelling provides more specific surface area for

DOI: 10.1021/acssuschemeng.6b03191
ACS Sustainable Chem. Eng. 2017, 5, 3346−3352

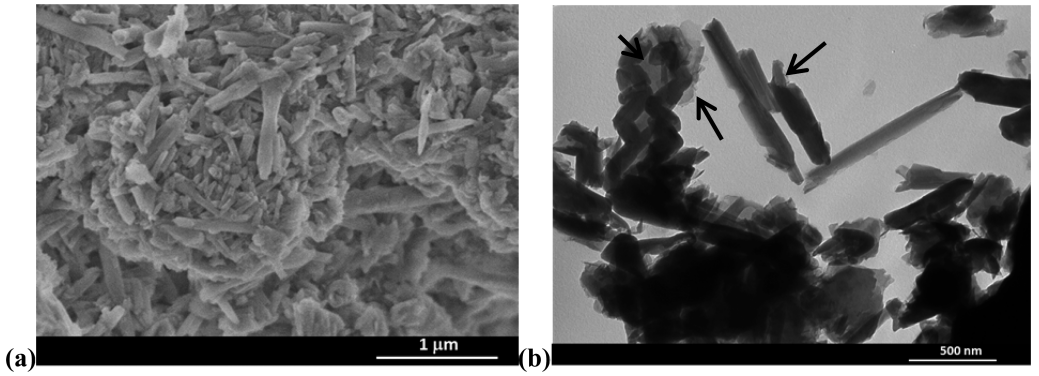

Figure 3. (a) SEM and (b) TEM images of HNT-CDs (40%) nanosponge hybrid.

Table 2. Textural Parameters Determined by N_2 Adsorption/Desorption Measurements for p-HNT and HNT-CD Nanosponge Hybrid

	surface area, S_{BET} (m^2 g^{-1})	total pore volume (cm^3 g^{-1})	average pore size (nm)
p-HNT[34]	22.1	0.06	9.3
HNT-CDs	19.9	0.29	85.2

adsorption, wettability and swelling are presumed to facilitate the adsorption of target molecules or ions. Therefore, it is essential to measure swelling of a polymer in an aqueous medium before its application as adsorbent. The swelling ratio of the HNT-CDs (40%) nanosponge hybrid is 91.2 ± 1.6%. The reduction of the swelling ratio in comparison with some previously reported cyclodextrin polymers[36] could be due to the presence of HNT that increased cross-linking density through formation of covalent bonding within the cyclodextrin; as a consequence, HNTs could make the hybrid polymer network denser, blocking the passage of water from entering in the polymer.

Adsorption Measurements. The adsoption capacity of the new hybrid nanomaterials were evaluated by adsorption isotherm experiments using Rhodamine B (RB) as the dye model. In Figure 4 is reported the equilibrium amount of dye adsorbed into the clay (Q_e, mol g^{-1}) as a function of the equilibrium dye concentration in solution (C_e, mol L^{-1}). First of all, it can be observed that the amount of adsorbed dye

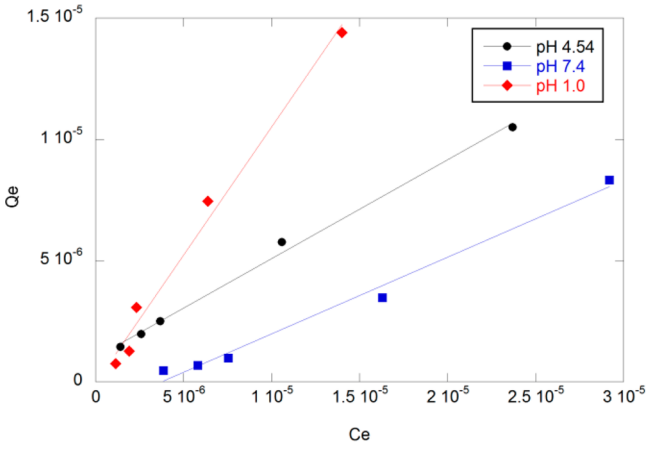

Figure 4. Adsorption isotherms of RB on HNT-CD nanosponge hybrid in HCl 0.1 N, acetate buffer pH 4.54, and phosphate buffer pH 7.4.

increases on increasing the equilibrium dye concentration, and it is considerably lower at the higher pH (Figure 4). This could be explained as follows: HNT presents a negative outer surface in a wide pH range. Therefore, in acidic pH media an electrostatic attraction between the negatively charged nanosponge hybrid and positively charged RB would take place. On the contrary, for pH values up to 7.4, RB mainly exists in zwitterion forms forming dimers[37] which are unable to interact with the HNT surfaces, and therefore, the dye can be encapsulated mainly into CD cavities decreasing the adsorption efficiency.

Both the Langmuir and the Freundlich models were used to analyze the experimental data. The obtained results are reported in Table 3. As shown, the adsorption data are better fitted by the Freundlich model suggesting the heterogeneity of the polymer and multimolecular layer adsorption. The value of n is larger than 1 in acidic solution, which indicates the favorable nature of adsorption and a physical process. While the n value less than 1 obtained in a neutral medium indicates that the adsorption bond becomes weak, unfavorable adsorption takes place, as a result of the decrease in adsorption capacity.[38]

For comparison, we studied the adsorption of RB on pristine HNT (p-HNT). In all cases, we observed a decrease in the RB adsorption efficiency with respect to the HNT-CD hybrids (SI). In addition, the adsorption data are better fitted by the Langmuir model at pH 7.4; furthermore, both models are not applicable for data at pH 4.54.

To well understand the adsorption mechanisms, kinetics of Rhodamine B adsorption onto HNT-CDs nanosponge hybrids, in the best pH conditions, were investigated (SI). It was found that the adsorption amount increases rapidly in the first 100 min and then slows until the sorption reached equilibrium. The beginning rapid adsorption of RB is due to the existence of a large number of sorption sites on the surface of HNT-CDs nanosponge hybrids (HNT and CDs cavities, interstitial channels). As the surface active sites are occupied, the adsorption rates slow down and finally reach the adsorption equilibrium.

The kinetic data were fitted by first-order, second-order, intraparticle diffusion, and double exponential (DEM) models (Table S1). It was found that the experimental data are better fitted by the DEM model (Table 4). According to the literature, the DEM mode describes a process where the adsorbent offers two different types of adsorption sites.[39] Therefore, it could be possible that rapid adsorption equilibration occurs within a few minutes onto the HNT external surface, whereas on the inner cyclodextrin core, adsorption occurs more slowly.

DOI: 10.1021/acssuschemeng.6b03191
ACS Sustainable Chem. Eng. 2017, 5, 3346−3352

Table 3. Parameters of Langmuir and Freundlich Isotherm Models for RB Adsorption on HNT-CDs Nanosponge Hybrids

		Langmuir			Freundlich		
		$Q_e = \frac{K_L Q_m C_e}{1 + K_L C_e}$			$Q_e = K_F C_e^{1/n}$		
pH		Q_m (mol g^{-1})	K_L (L mol^{-1})	R^2	K_F (mol g^{-1} (mol L^{-1})$^{1/n}$)	n	R^2
1.00	HNT-CDs (20%)	$(2.7 \pm 1.5) \times 10^{-5}$	$(7 \pm 6) \times 10^5$	0.965	0.08 ± 0.06	1.3 ± 0.1	0.996
	HNT-CDs (40%)	$(2.0 \pm 0.1) \times 10^{-5}$	$(3 \pm 2) \times 10^5$	0.964	0.3 ± 0.1	1.01 ± 0.03	0.977
4.54	HNT-CDs (20%)	$(2.5 \pm 0.4) \times 10^{-5}$	$(3 \pm 1) \times 10^5$	0.994	0.05 ± 0.01	1.26 ± 0.05	0.997
	HNT-CDs (40%)	$(6 \pm 4) \times 10^{-5}$	$(8 \pm 6) \times 10^4$	0.991	0.10 ± 0.06	1.13 ± 0.07	0.994
7.40	HNT-CDs (20%)	na[a]	na	na	86 ± 40	0.65 ± 0.02	0.999
	HNT-CDs (40%)	na	na	na	2.2 ± 1.9	0.80 ± 0.05	0.994

[a]na: Langmuir model is not successful.

Table 4. Adsorption Kinetic Parameters of RB onto HNT-CDs Nanosponge Hybrids

	DEM				
	$Q_T = Q_e'(1 - e^{k't}) + Q_e''(1 - e^{k''t})$				
	Q_e' (10^{-6} M)	k' (min^{-1})	Q_e''(10^{-6} M)	k'' (min^{-1})	R^2
20%	3.91 ± 0.02	0.083 ± 0.003	1.61 ± 0.02	$(3.4 \pm 0.01) \times 10^{-3}$	0.994
40%	3.73 ± 0.02	0.8 ± 0.1	1.61 ± 0.02	$(1.35 \pm 0.03) \times 10^{-2}$	0.981

Finally, in order to determine the effect of temperature on RB adsorption, experiments were conducted at 277, 298, 310, and 331 K. The adsorption process was favorable at lower temperature, and RB molecules were orderly adsorbed on the surface of HNT-CDs nanosponge and into CD cavities. The thermodynamic parameters were calculated by means of the van't Hoff equation and are listed in Table 5. The obtained data further confirm that the material shows better adsorption efficiency in an acidic medium with respect to the neutral one.

Table 5. Thermodynamic Parameters at Different Temperatures

pH	T (K)	$\Delta G°$,[a] (kJ mol^{-1})	ΔH (kJ mol^{-1})	ΔS (J mol^{-1})
4.54	277	−88.31	−100.71	−44.76
	298	−87.37		
	310	−86.83		
	331	−85.89		
7.40	277	1.87	−37.19	−141

[a]Obtained from the Langmuir model.

In order to evaluate the performance of the obtained HNT-CD hybrid polymers, additional adsorption experiments were performed to determine the adsorption capacity of the hybrid for six cationic and anionic dyes (SI), under different pH values, namely, 1.0, 4.54, and 7.4 (Figure 5). In general, the synthesized materials show higher adsorption capacity than p-HNT (Figure S8 and Table S2) as a consequence of the introduction of CD moieties and the formation of a network.

It was found that HNT-CDs hybrids, in all pH values investigated, showed high adsorption capacity for cationic dyes. In particular, methylene blue (MB) and toluidine blue (TB) are quantitatively adsorbed, while only 70% of RB is adsorbed at the best pH value. These differences could be due to the small steric hindrance of MB and TB with respect to RB.

Anionic dyes are poorly adsorbed from the polymer, probably due to the presence of electrostatic repulsions between the negatively charged halloysite external surface and the dyes. The small amount of these dyes adsorbed could

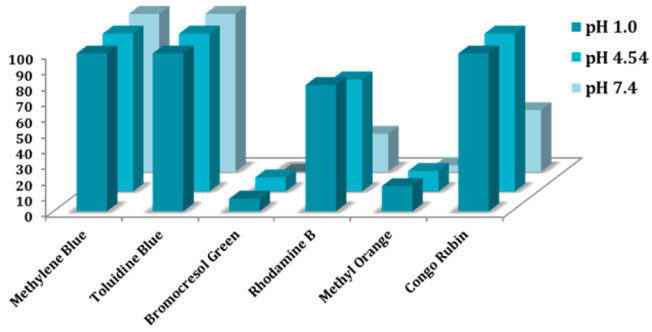

Figure 5. Adsorption capacities of HNT-CD hybrid polymer for the different dyes at pH 1, 4.54, and 7.4.

selectively interact with positively charged HNT lumen. However, in these cases, the best adsorption is obtained at pH 4.54. The anionic dyes, indeed, turn from a neutral to a largely delocalized anionic form at around pH 4; therefore, they can interact with the nanomaterial in their partly cationic form.[40]

Surprisingly, the nanomaterial showed good adsorption capacity for the anionic dye congo Rubin (CR) at acidic pH values. This could be explained by a difference in binding mechanism of halloysite to the anionic dyes and a strong interaction between CR and HNT.[41] In addition, the formation of inclusion complexes between CR and β-CD occurs.[42] At lower pH, the sulfonate ions of CR can be neutralized, and the complexing effect between neutral CR and the cavity of β-CD is strengthened, thereby promoting adsorption of CR.

The obtained results show that HNT-CDs nanosponge hybrids could be used as a good nanoadsorbent for selective adsorption of cationic dyes with respect to the anionic ones in a wide pH range.

For comparison, in Table 6 are reported the adsorption capacities of MB on the HNT-CD (40%) hybrid and those obtained with other adsorbents.

DOI: 10.1021/acssuschemeng.6b03191
ACS Sustainable Chem. Eng. 2017, 5, 3346−3352

Table 6. Adsorption Capacities of MB for Some Adsorbents

adsorbent	adsorption capacity (mg g^{-1})	ref
p-HNT	84.32	43
titania	5.98	23
zeolite	16.37	24
NaOH-treated kaolin	20.49	22
titanate nanotubes	133.30	44
β-cyclodextrin cross-linked by citric acid	105.00	45
HNT-CD (40%) hybrid	226	this work

The results demonstrated that the HNT-CD hybrid nanosponges could be employed as promising adsorbents for removal of organic dyes from wastewater.

CONCLUSIONS

New hybrid organic−inorganic nanosponges based on halloysite nanotubes and cyclodextrins were successful synthesized by microwave irradiation in solvent-free conditions. In particular, by combining the starting scaffolds in different ratios, it was possible to obtain two nanosponges with different amounts of organic moieties that possess some nonreacted allyl groups that can be subjected to further functionalizations. The structure and morphology of the hybrid materials were extensively investigated by means of several techniques such as thermogravimetric analysis, TEM and SEM investigations, DLS and ζ-potential measurements, and FT-IR spectroscopy. BET measurements and swelling investigations highlighted the presence of a hyper-reticulated network and the possible presence of an interstitial channel that could be useful for future applications. The feasibility of the material as a decontaminant of wastewater was investigated by studying its adsorption capacity toward an organic dye, Rhodamine B. Adsorption experiments evidenced that the adsorption capacity is strictly influenced by the pH of the medium, and the presence of cyclodextrin in the hybrid enhances the adsorption ability of halloysite. The performance of the hybrid nanosponge was also evaluated toward different cationic and anionic dyes, and the obtained results showed that HNT-CDs nanosponge hybrids are good nanoadsorbents for selective adsorption of cationic dyes with respect to the anionic ones in a wide pH range. In conclusion, we think that the nanomaterial prepared combines the properties of both halloysite and cyclodextrin, and therefore, it puts forward the use of halloysite in the bioremediation field.

ASSOCIATED CONTENT

Supporting Information

The Supporting Information is available free of charge on the ACS Publications website at DOI: 10.1021/acssuschemeng.6b03191.

Experimental details, N_2 adsorption/desorption isotherm, adsorption isotherms, adsorption kinetics and kinetic parameters, temperature-dependent adsorption, structure of the investigated dyes, and adsorption capacities of p-HNT (PDF). (PDF)

AUTHOR INFORMATION

Corresponding Authors

*E-mail: giuseppe.lazzara@unipa.it (G. Lazzara).
*E-mail: serena.riela@unipa.it (S. Riela).

ORCID

Serena Riela: 0000-0001-8705-8763

Author Contributions

The manuscript was written through contributions of all authors. All authors have given approval to the final version of the manuscript.

Notes

The authors declare no competing financial interest.

ACKNOWLEDGMENTS

The work was financially supported by the University of Palermo (Italy), FIRB 2012 (prot. RBFR12ETL5) and PON-TECLA (PON03PE_00214_1).

REFERENCES

(1) Ma, T.-Y.; Liu, L.; Yuan, Z.-Y. Direct Synthesis of Ordered Mesoporous Carbons. *Chem. Soc. Rev.* **2013**, *42* (9), 3977−4003.
(2) Salem, S.; Salem, A.; Agha Babaei, A. Preparation and Characterization of Nano Porous Bentonite for Regeneration of Semi-Treated Waste Engine Oil: Applied Aspects for Enhanced Recovery. *Chem. Eng. J.* **2015**, *260*, 368−376.
(3) Bakare, I. A.; Muraza, O.; Taniguchi, T.; Tago, T.; Nasser, G.; Yamani, Z. H.; Masuda, T. Steam-Assisted Catalytic Cracking of N-Hexane over La-Modified Mtt Zeolite for Selective Propylene Production. *J. Anal. Appl. Pyrolysis* **2015**, *116*, 272−280.
(4) Fakhrullina, G. I.; Akhatova, F. S.; Lvov, Y. M.; Fakhrullin, R. F. Toxicity of Halloysite Clay Nanotubes in Vivo: A Caenorhabditis Elegans Study. *Environ. Sci.: Nano* **2015**, *2* (1), 54−59.
(5) Kryuchkova, M.; Danilushkina, A.; Lvov, Y.; Fakhrullin, R. Evaluation of Toxicity of Nanoclays and Graphene Oxide: In Vivo a Paramecium Caudatum Study. *Environ. Sci.: Nano* **2016**, *3* (2), 442−452.
(6) Bellani, L.; Giorgetti, L.; Riela, S.; Lazzara, G.; Scialabba, A.; Massaro, M. Ecotoxicity of Halloysite Nanotube−Supported Palladium Nanoparticles in Raphanus Sativus L. *Environ. Toxicol. Chem.* **2016**, *35* (10), 2503−2510.
(7) Lvov, Y.; Wang, W.; Zhang, L.; Fakhrullin, R. Halloysite Clay Nanotubes for Loading and Sustained Release of Functional Compounds. *Adv. Mater.* **2016**, *28* (6), 1227−1250.
(8) Lvov, Y. M.; DeVilliers, M. M.; Fakhrullin, R. F. The Application of Halloysite Tubule Nanoclay in Drug Delivery. *Expert Opin. Drug Delivery* **2016**, *13* (7), 977−986.
(9) Biddeci, G.; Cavallaro, G.; Di Blasi, F.; Lazzara, G.; Massaro, M.; Milioto, S.; Parisi, F.; Riela, S.; Spinelli, G. Halloysite Nanotubes Loaded with Peppermint Essential Oil as Filler for Functional Biopolymer Film. *Carbohydr. Polym.* **2016**, *152*, 548−557.
(10) Fan, L.; Zhang, J.; Wang, A. In Situ Generation of Sodium Alginate/Hydroxyapatite/Halloysite Nanotubes Nanocomposite Hydrogel Beads as Drug-Controlled Release Matrices. *J. Mater. Chem. B* **2013**, *1* (45), 6261−6270.
(11) Liu, M.; Chang, Y.; Yang, J.; You, Y.; He, R.; Chen, T.; Zhou, C. Functionalized Halloysite Nanotube by Chitosan Grafting for Drug Delivery of Curcumin to Achieve Enhanced Anticancer Efficacy. *J. Mater. Chem. B* **2016**, *4* (13), 2253−2263.
(12) Massaro, M.; Piana, S.; Colletti, C. G.; Noto, R.; Riela, S.; Baiamonte, C.; Giordano, C.; Pizzolanti, G.; Cavallaro, G.; Milioto, S.; Lazzara, G. Multicavity Halloysite-Amphiphilic Cyclodextrin Hybrids for Co-Delivery of Natural Drugs into Thyroid Cancer Cells. *J. Mater. Chem. B* **2015**, *3* (19), 4074−4081.
(13) Massaro, M.; Riela, S.; Baiamonte, C.; Blanco, J. L. J.; Giordano, C.; Lo Meo, P.; Milioto, S.; Noto, R.; Parisi, F.; Pizzolanti, G.; Lazzara, G. Dual Drug-Loaded Halloysite Hybrid-Based Glycocluster for Sustained Release of Hydrophobic Molecules. *RSC Adv.* **2016**, *6* (91), 87935−87944.
(14) Massaro, M.; Amorati, R.; Cavallaro, G.; Guernelli, S.; Lazzara, G.; Milioto, S.; Noto, R.; Poma, P.; Riela, S. Direct Chemical Grafted

DOI: 10.1021/acssuschemeng.6b03191
ACS Sustainable Chem. Eng. 2017, 5, 3346−3352

Curcumin on Halloysite Nanotubes as Dual-Responsive Prodrug for Pharmacological Applications. *Colloids Surf., B* **2016**, *140*, 505−513.
(15) Massaro, M.; Riela, S.; Cavallaro, G.; Colletti, C. G.; Milioto, S.; Noto, R.; Parisi, F.; Lazzara, G. Palladium Supported on Halloysite-Triazolium Salts as Catalyst for Ligand Free Suzuki Cross-Coupling in Water under Microwave Irradiation. *J. Mol. Catal. A: Chem.* **2015**, *408*, 12−19.
(16) Massaro, M.; Schembri, V.; Campisciano, V.; Cavallaro, G.; Lazzara, G.; Milioto, S.; Noto, R.; Parisi, F.; Riela, S. Design of PNIPAAM Covalently Grafted on Halloysite Nanotubes as a Support for Metal-Based Catalysts. *RSC Adv.* **2016**, *6* (60), 55312−55318.
(17) Peng, Q.; Liu, M.; Zheng, J.; Zhou, C. Adsorption of Dyes in Aqueous Solutions by Chitosan-Halloysite Nanotubes Composite Hydrogel Beads. *Microporous Mesoporous Mater.* **2015**, *201* (C), 190−201.
(18) Massaro, M.; Riela, S.; Cavallaro, G.; Colletti, C. G.; Milioto, S.; Noto, R.; Lazzara, G. Ecocompatible Halloysite/Cucurbit[8]Uril Hybrid as Efficient Nanosponge for Pollutants Removal. *ChemistrySelect* **2016**, *1* (8), 1773−1779.
(19) Shao, X.; Li, C.; Chen, S.; Yao, K.; Yao, M. Functional Two-Dimensional Organic−Inorganic Hybrid Materials with Regular Peptides. *Colloids Surf., A* **2013**, *424*, 66−73.
(20) Mahmoud, M. E.; Hafez, O. F.; Osman, M. M.; Yakout, A. A.; Alrefaay, A. Hybrid Inorganic/Organic Alumina Adsorbents-Functionalized-Purpurogallin for Removal and Preconcentration of Cr(Iii), Fe(Iii), Cu(Ii), Cd(Ii) and Pb(Ii) from Underground Water. *J. Hazard. Mater.* **2010**, *176* (1−3), 906−912.
(21) Liang, X.; Lu, Y.; Li, Z.; Yang, C.; Niu, C.; Su, X. Bentonite/Carbon Composite as Highly Recyclable Adsorbents for Alkaline Wastewater Treatment and Organic Dye Removal. *Microporous Mesoporous Mater.* **2017**, *241*, 107−114.
(22) Ghosh, D.; Bhattacharyya, K. G. Adsorption of Methylene Blue on Kaolinite. *Appl. Clay Sci.* **2002**, *20* (6), 295−300.
(23) Fetterolf, M. L.; Patel, H. V.; Jennings, J. M. Adsorption of Methylene Blue and Acid Blue 40 on Titania from Aqueous Solution. *J. Chem. Eng. Data* **2003**, *48* (4), 831−835.
(24) Han, R.; Zhang, J.; Han, P.; Wang, Y.; Zhao, Z.; Tang, M. Study of Equilibrium, Kinetic and Thermodynamic Parameters About Methylene Blue Adsorption onto Natural Zeolite. *Chem. Eng. J.* **2009**, *145* (3), 496−504.
(25) Massaro, M.; Riela, S.; Lo Meo, P.; Noto, R.; Cavallaro, G.; Milioto, S.; Lazzara, G. Functionalized Halloysite Multivalent Glycocluster as a New Drug Delivery System. *J. Mater. Chem. B* **2014**, *2* (44), 7732−7738.
(26) Massaro, M.; Riela, S.; Cavallaro, G.; Gruttadauria, M.; Milioto, S.; Noto, R.; Lazzara, G. Eco-Friendly Functionalization of Natural Halloysite Clay Nanotube with Ionic Liquids by Microwave Irradiation for Suzuki Coupling Reaction. *J. Organomet. Chem.* **2014**, *749*, 410−415.
(27) Liang, W.; Yang, C.; Zhou, D.; Haneoka, H.; Nishijima, M.; Fukuhara, G.; Mori, T.; Castiglione, F.; Mele, A.; Caldera, F.; Trotta, F.; Inoue, Y. Phase-Controlled Supramolecular Photochirogenesis in Cyclodextrin Nanosponges. *Chem. Commun.* **2013**, *49* (34), 3510−3512.
(28) Wei, X.; Liang, W.; Wu, W.; Yang, C.; Trotta, F.; Caldera, F.; Mele, A.; Nishimoto, T.; Inoue, Y. Solvent- and Phase-Controlled Photochirogenesis. Enantiodifferentiating Photoisomerization of (Z)-Cyclooctene Sensitized by Cyclic Nigerosylnigerose-Based Nanosponges Crosslinked by Pyromellitate. *Org. Biomol. Chem.* **2015**, *13* (10), 2905−2912.
(29) Lo Meo, P.; Lazzara, G.; Liotta, L.; Riela, S.; Noto, R. Cyclodextrin-Calixarene Co-Polymers as a New Class of Nanosponges. *Polym. Chem.* **2014**, *5* (15), 4499−4510.
(30) Riela, S.; Lazzara, G.; Lo Meo, P.; Guernelli, S.; D'Anna, F.; Milioto, S.; Noto, R. Microwave-Assisted Synthesis of Novel Cyclodextrin−Cucurbituril Complexes. *Supramol. Chem.* **2011**, *23* (12), 819−828.
(31) Lazzara, G.; Milioto, S. Dispersions of Nanosilica in Biocompatible Copolymers. *Polym. Degrad. Stab.* **2010**, *95* (4), 610−617.
(32) Massaro, M.; Riela, S.; Guernelli, S.; Parisi, F.; Lazzara, G.; Baschieri, A.; Valgimigli, L.; Amorati, R. A Synergic Nanoantioxidant Based on Covalently Modified Halloysite-Trolox Nanotubes with Intra-Lumen Loaded Quercetin. *J. Mater. Chem. B* **2016**, *4* (13), 2229−2241.
(33) Del Buffa, S.; Grifoni, E.; Ridi, F.; Baglioni, P. The Effect of Charge on the Release Kinetics from Polysaccharide−Nanoclay Composites. *J. Nanopart. Res.* **2015**, *17* (3), 146.
(34) Pasbakhsh, P.; Churchman, G. J.; Keeling, J. L. Characterisation of Properties of Various Halloysites Relevant to Their Use as Nanotubes and Microfibre Fillers. *Appl. Clay Sci.* **2013**, *74*, 47−57.
(35) Massaro, M.; Cina, V.; Labbozzetta, M.; Lazzara, G.; Lo Meo, P.; Poma, P.; Riela, S.; Noto, R. Chemical and Pharmaceutical Evaluation of the Relationship between Triazole Linkers and Pore Size on Cyclodextrin-Calixarene Nanosponges Used as Carriers for Natural Drugs. *RSC Adv.* **2016**, *6* (56), 50858−50866.
(36) Jalalvandi, E.; Cabral, J.; Hanton, L. R.; Moratti, S. C. Cyclodextrin-Polyhydrazine Degradable Gels for Hydrophobic Drug Delivery. *Mater. Sci. Eng., C* **2016**, *69*, 144−153.
(37) Yang, C.; Wu, S.; Cheng, J.; Chen, Y. Indium-Based Metal-Organic Framework/Graphite Oxide Composite as an Efficient Adsorbent in the Adsorption of Rhodamine B from Aqueous Solution. *J. Alloys Compd.* **2016**, *687*, 804−812.
(38) Gereli, G.; Seki, Y.; Murat Kuşoğlu, İ.; Yurdakoç, K. Equilibrium and Kinetics for the Sorption of Promethazine Hydrochloride onto K10 Montmorillonite. *J. Colloid Interface Sci.* **2006**, *299* (1), 155−162.
(39) Qiu, H.; Lv, L.; Pan, B.-c.; Zhang, Q.-j.; Zhang, W.-m.; Zhang, Q.-x. Critical Review in Adsorption Kinetic Models. *J. Zhejiang Univ., Sci., A* **2009**, *10* (5), 716−724.
(40) Russo, M.; Saladino, M. L.; Chillura Martino, D.; Lo Meo, P.; Noto, R. Polyaminocyclodextrin Nanosponges: Synthesis, Characterization and Ph-Responsive Sequestration Abilities. *RSC Adv.* **2016**, *6* (55), 49941−49953.
(41) Chen, H.; Zhao, J.; Wu, J.; Yan, H. Selective Desorption Characteristics of Halloysite Nanotubes for Anionic Azo Dyes. *RSC Adv.* **2014**, *4* (30), 15389−15393.
(42) Yu, L.; Xue, W.; Cui, L.; Xing, W.; Cao, X.; Li, H. Use of Hydroxypropyl-B-Cyclodextrin/Polyethylene Glycol 400, Modified Fe3o4 Nanoparticles for Congo Red Removal. *Int. J. Biol. Macromol.* **2014**, *64*, 233−239.
(43) Zhao, M.; Liu, P. Adsorption Behavior of Methylene Blue on Halloysite Nanotubes. *Microporous Mesoporous Mater.* **2008**, *112* (1−3), 419−424.
(44) Xiong, L.; Yang, Y.; Mai, J.; Sun, W.; Zhang, C.; Wei, D.; Chen, Q.; Ni, J. Adsorption Behavior of Methylene Blue onto Titanate Nanotubes. *Chem. Eng. J.* **2010**, *156* (2), 313−320.
(45) Zhao, D.; Zhao, L.; Zhu, C.-S.; Huang, W.-Q.; Hu, J.-L. Water-Insoluble B-Cyclodextrin Polymer Crosslinked by Citric Acid: Synthesis and Adsorption Properties toward Phenol and Methylene Blue. *J. Inclusion Phenom. Mol. Recognit. Chem.* **2009**, *63* (3), 195−201.

DOI: 10.1021/acssuschemeng.6b03191
ACS Sustainable Chem. Eng. 2017, 5, 3346−3352